Structures, Vibrational Spectra, and Relative Energetics of CH_3BrO_3 Isomers

Sujata Guha and Joseph S. Francisco*

Department of Chemistry and Department of Earth & Atmospheric Sciences, Purdue University, West Lafayette, Indiana 47907-1393

Received: November 9, 1999; In Final Form: January 26, 2000

The geometries, vibrational spectra, and relative energetics of CH_3BrO_3 isomers have been examined using the B3LYP method in conjunction with various basis sets. The CH_3OBrO_2 isomer is found to be the lowest energy structure among the isomers, with an estimated heat of formation of 10.6 kcal mol^{-1}, at 0 K, as determined from G2 theory. The next lowest energy isomer is CH_3OOOBr, which lies 5.6 kcal mol^{-1} above CH_3OBrO_2. The isomers with higher energies are CH_3OOBrO and CH_3BrO_3. We have examined the implication of the formation of the CH_3BrO_3 isomers from the atmospheric cross-reactions of the CH_3O_2 and BrO radical species.

I. Introduction

Bromine is the most effective halogen species that participates in efficient catalytic cycles leading to the destruction of ozone. Although bromine-containing compounds are much less abundant than chlorine-containing compounds in the stratosphere, it has been estimated that the chemistry involving bromine species is responsible for ∼25% of the loss of ozone in Antarctica,[1] and up to 40% of ozone loss during winter in the Arctic region.[2] The efficiency of bromine in destroying ozone is greatly enhanced by its synergistic coupling with chlorine compounds, leading to the production of bromine and chlorine atoms.[3]

$$BrO + ClO \rightarrow Br + Cl + O_2 \quad (1)$$

The most abundant bromine-containing source gas is methyl bromide (CH_3Br), present mainly due to oceanic biological processes. Methyl bromide is used for fumigation, has a high ozone depletion potential (ODP), and is scheduled to be phased out in developed countries by the year 2010.[4] Other important source gases of bromine that reach the stratosphere after emission from the troposphere include tetrabromobisphenol A and trifluoromethyl bromide, used as fire retardants and refrigerants.

The coupling of bromine oxides with other radical families is critical as such processes lead to destruction of the ozone layer. A very important category of coupling reaction of bromine oxides is those with the HO_x species (such as HO and HO_2 radicals), particularly the reaction between BrO and HO_2 radicals. This process increases the recycling of bromine radicals, and is efficient in regions with significant hydroxyl radical concentrations. Vogt et al.[5] suggested that ozone is partly depleted in the marine boundary layer through catalytic cycles involving BrO and HO_2 radicals which have been investigated in the laboratory by Poulet et al.,[6] Larichev et al.,[7] and Elrod et al.[8]

$$Br + O_3 \rightarrow BrO + O_2 \quad (2)$$

$$BrO + HO_2 \rightarrow HOBr + O_2 \quad (3)$$

$$HOBr + h\nu \rightarrow OH + Br \quad (4)$$

$$OH + O_3 \rightarrow HO_2 + O_2 \quad (5)$$

$$\text{Net: } 2O_3 \rightarrow 3O_2 \quad (6)$$

HOBr formed in reaction 3 is rapidly converted into active bromine via photodissociation in the stratosphere. Vogt et al.[5] and Fan and Jacob[9] suggested that the conversion of HOBr into bromine atom could occur on the surface of aerosols.

It has been suggested that, similar to the $BrO + HO_2$ reaction, the $BrO + CH_3O_2$ reaction may be involved in the bromine-catalyzed oxidation of methane as speculated in a modeling study of the chemistry of the lower stratosphere. In fact, a similar reaction between CH_3O_2 and ClO radicals has been supposed to participate in ozone depleting cycles under ozone hole conditions.[10] The $BrO + CH_3O_2$ reaction has also been considered in catalytic cycles which could result from the halogen released from sea salt aerosol in the marine boundary layer.[11] As in reaction 3, BrO may be converted into HOBr via recycling into active bromine, provided the $BrO + CH_3O_2$ reaction proceeds via the channel:[11]

$$BrO + CH_3O_2 \rightarrow HOBr + CH_2O_2 \qquad \Delta H = (-1.6 \pm 5.4) \text{ kcal mol}^{-1} \quad (7a)$$

Aranda et al.[11] suggested that an additional possible channel not existing for reaction 3 is the conversion of BrO into Br:

$$BrO + CH_3O_2 \rightarrow Br + CH_3O + O_2 \qquad \Delta H = (-0.9 \pm 4.4) \text{ kcal mol}^{-1} \quad (7b)$$

In this paper we examine the possibility of the different CH_3BrO_3 isomers that could be formed from the reaction occurring between CH_3O_2 and BrO radicals.

$$BrO + CH_3O_2 \rightarrow [CH_3BrO_3]^* \rightarrow \text{products} \quad (7c)$$

There have been no previous computational studies on any CH_3BrO_3 species, and no experimental studies have been reported that have isolated the intermediate. It is important to consider the possible existence of such an intermediate and its isomers, because the CH_3BrO_3 intermediate, if present in a stable form, could act as a reservoir of inorganic bromine in the stratosphere. There are four types of plausible connectivities for the CH_3BrO_3 isomers, namely, (1) CH_3OOOBr, (2) CH_3OOBrO, (3) CH_3OBrO_2, and (4) CH_3BrO_3. In our present work we employ density functional theory (DFT) to examine the minimum-energy structural forms for the CH_3BrO_3 species. Harmonic vibrational frequencies along with infrared intensities are presented to aid

10.1021/jp993964p CCC: $19.00
Published on Web 03/22/2000

in their spectroscopic characterization. The heats of formation of the CH_3BrO_3 species are also estimated to determine the relative order of stability among the species. Such a study should shed light on the intimate details of the $BrO_x + CH_3O_x$ reaction chemistry and the possible involvement of the CH_3BrO_3 intermediates.

II. Computational Methods

Ab initio molecular orbital calculations were performed using the GAUSSIAN 94 program.[12] All equilibrium geometrical parameters were fully optimized, using Schlegel's method, to better than 0.001 Å for bond distances and 0.10° for bond angles with a self-consistent field (SCF) convergence of at least 10^{-9} on the density matrix. The residual root-mean-square (rms) force is less than 10^{-4} au. The B3LYP (Becke's nonlocal three-parameter exchange with the Lee−Yang−Parr correlation functional) method[13] was used with the 6-31G(d), 6-311G(d,p), 6-311G(2d,2p), 6-311G(2df,2p), and 6-311++G(3df,3pd) basis sets. The harmonic vibrational frequencies and intensities of all the isomers were calculated at the B3LYP level of theory in conjugation with the large 6-311++G(3df,3pd) basis set, using the geometrical parameters calculated at the B3LYP theory level with the same basis set. The heats of formation of CH_3OOOBr were determined using an isodesmic reaction scheme, and compared to the heats of formation estimated using the G1 and G2 theories.[14,15]

III. Results and Discussion

A. Structures and Vibrational Frequencies of CH_3BrO_3 Isomers. To identify the lowest energy isomer on the hypersurface of the CH_3BrO_3 potential energy, we performed calculations at various levels of theory. Four local minimum-energy structures were located. The optimized structural parameters are provided in Table 1 and illustrated in Figure 1. The geometries at the HF/6-31G(d) and MP2/6-31G(d) levels of theory, obtained using the G2 method, are also provided in the table.

The ground-state geometry for CH_3OOOBr is provided in Table 1. From computations, the minimum-energy structure for CH_3OOOBr is skewed (Figure 1a). The HCOO dihedral angles range from −67.4 to 174.6° at the B3LYP/6-311++G(3df,3pd) level of theory. The COOO′ dihedral angle is predicted to be 71.5°, while the OOO′Br dihedral angle is 79.9°. It is interesting to compare the O−O and O−O′ bond lengths in CH_3OOOBr (1.430 and 1.375 Å, respectively) with the O−O and O−O′ bond lengths in the stratospherically important HOOOBr molecule (1.425 and 1.3781 Å, respectively).[16] The bonding between the two species is quite similar. However, the H−O bond, present in HOOOBr, is absent in CH_3OOOBr, since in the latter species, the carbon atom is linked to oxygen, instead of a hydrogen atom. Using the B3LYP method, the COO and OO′Br angles in CH_3OOOBr are predicted to be 109.3° and 112.7°, respectively. The OOO′ angle (109.8°) is smaller than the OO′Br angle (112.7°) due to the greater amount of repulsion between the lone pairs of electrons on bromine with those on oxygen, compared to the repulsion occurring between the lone pairs of electrons on the two oxygen atoms. There is poor overlap between the 3d orbitals of the large bromine atom with the 2p orbital of the oxygen atom compared to the overlap between the orbitals of two equal-sized oxygen atoms. Thus, the O′-Br bond length is larger (1.905 Å) than the O−O and O−O′ bond lengths in CH_3OOOBr.

The second isomeric form we considered is CH_3OOBrO. This, too, is a skewed structure but with oxygen as the terminal atom (Figure 1b). The dihedral angle between the COOBr atoms is 92.2°, while that between the OOBrO′ atoms is 77.4°. The OBrO′ angle (110.0°) is a little narrower than the OOBr angle (112.2°). As in the case of CH_3OOOBr, the COO angle (108.9°) in CH_3OOBrO is smaller than the OOBr angle (112.2°), due to the greater degree of repulsion between the two lone pairs of electrons on bromine with those on the oxygen atom. The O−Br bond distance predicted at the B3LYP/6-311++G(3df,3pd) level of theory is 1.926 Å and agrees quite well with the O−Br lengths computed using the B3LYP level of theory in conjunction with other basis sets. For different basis sets used, the O−Br bond lengths are greater than the Br−O′ bond lengths. The lone pairs of electrons on the terminal oxygen atom sometimes tend to enter into resonance with the Br−O′ bond pairs, due to which the Br−O′ bond attains a partial double-bond character. Such resonance effect is not observed with the oxygen atoms that are sandwiched between the carbon and the bromine atoms. Thus the Br−O′ bond with its partial double-bond character is shorter (1.666 Å) than the O−Br bond (1.926 Å). The O−O bond length in CH_3OOBrO (1.408 Å) is comparable to the O−O bond length in $HOOBrO$[16] (1.415 A). The OOBr and OBrO′ angles in CH_3OOBrO and $HOOBrO$ are also very similar. The HOO angle, present in $HOOBrO$, is absent in CH_3OOBrO.

The third isomeric form is CH_3OBrO_2 (Figure 1c). The O′−Br bond (1.850 Å) is longer than the bonds formed between bromine and the terminal oxygen atoms. This is because the lone pairs of electrons on the terminal oxygen atoms enter into partial resonance with their immediate bonding electron neighbors, thus rendering a partial double-bond character to the terminal Br−O bonds. The C−O bond length in CH_3OBrO_2 (1.436 Å) is a bit larger than the C−O bond lengths in CH_3OOOBr and CH_3OOBrO, while the C−H bond lengths between the three species are quite similar. The O′−Br and Br−O bond lengths between CH_3OBrO_2 and $HOBrO_2$[16] are also comparable.

The fourth isomeric form is CH_3BrO_3, with the three oxygen atoms forming the base of a pyramid. The Br−O bond in CH_3BrO_3 is the shortest among the terminal Br−O bonds in the other isomers. This is due to the resonance associated with the Br═O multiple bonding characteristics in CH_3BrO_3. Such an effect does not occur for CH_3OOOBr and occurs only for the terminal oxygen atoms of CH_3OOBrO and CH_3OBrO_2. Resonance plays a much stronger role in CH_3BrO_3 than it does in CH_3OOBrO and CH_3OBrO_2, making the Br═O bonded character more pronounced in CH_3BrO_3 than that in CH_3OOBrO and CH_3OBrO_2. The Br−O bond distance of 1.612 Å in CH_3BrO_3 at the B3LYP/6-311++G(3df,3pd) level of theory is shorter than the terminal Br−O′ bonds in CH_3OBrO_2 and CH_3OOBrO. The Br−O length in CH_3BrO_3 is a little larger than the Br−O length in $HBrO_3$ (1.604 Å). The H−Br bond, present in $HBrO_3$,[16] is absent in CH_3BrO_3.

The calculated vibrational frequencies and intensities for the four isomeric forms of CH_3BrO_3 are provided in Table 2. All vibrational frequencies noted in the table are obtained at the B3LYP level of theory using the large 6-311++G(3df,3pd) basis set.

In the prediction of the vibrational frequencies of CH_3OOOBr, the most intense band appears to be the C−O stretch (ν_9) at 991 cm^{-1}, while the least intense bands are the CH_3 symmetric deformation (ν_6), the CH_3 rock (ν_8), and the CH_3 twist (ν_{16}) at 1446, 1171, and 200 cm^{-1}, respectively. The harmonic frequencies of CH_3OOOBr are similar to those of $HOOOBr$.[16] However, the H−O stretch, HOO bend, and the HOOO torsion modes present in $HOOOBr$ are absent in CH_3OOOBr. Similarly the CH_3 symmetric and asymmetric stretches and deformation modes present in CH_3OOOBr are absent in $HOOOBr$. There

TABLE 1: Optimized Geometries (Ångstroms and Degrees) of CH_3BrO_3 Isomers

		levels of theory						
species	coordinates	HF/6-31G(d)	MP2/6-31G(d)	B3LYP/6-31G(d)	B3LYP/6-311G(d,p)	B3LYP/6-311G(2d,2p)	B3LYP/6-311G(2df,2p)	B3LYP/6-311++G(3df,3pd)
$CH_3OOO'Br$	*r*(CO)	1.411	1.432	1.429	1.430	1.429	1.426	1.427
	r(OO)	1.368	1.438	1.444	1.445	1.439	1.432	1.430
	r(OO′)	1.363	1.430	1.369	1.355	1.365	1.374	1.375
	r(O′Br)	1.825	1.898	1.943	1.968	1.942	1.911	1.905
	r(CH)	1.082	1.092	1.095	1.093	1.090	1.090	1.090
	r(CH′)	1.080	1.091	1.094	1.091	1.089	1.089	1.089
	r(CH″)	1.081	1.092	1.094	1.092	1.089	1.089	1.089
	∠(COO)	109.0	107.1	109.3	109.1	109.1	109.3	109.3
	∠(HCO)	110.3	110.5	111.1	110.9	110.9	111.0	110.8
	∠(H′CO)	104.8	103.7	103.5	103.6	103.8	104.0	103.9
	∠(H"CO)	110.7	110.6	111.1	111.1	111.1	111.2	111.1
	∠(OOO′)	107.9	107.4	110.0	110.4	110.1	109.9	109.8
	∠(OO′Br)	110.5	108.6	112.1	113.4	112.7	112.5	112.7
	∠(HCOO)	59.0	59.2	57.4	58.5	56.8	57.3	56.4
	∠(H′COO)	177.7	177.8	175.7	176.7	175.1	175.6	174.6
	∠(H"COO)	−63.7	−64.0	−66.5	−65.5	−67.1	−66.5	−67.4
	∠(COOO′)	83.6	75.6	65.4	68.7	68.4	70.3	71.5
	∠(OOO′Br)	81.8	75.8	76.2	81.5	80.3	79.2	79.9
CH_3OOBrO'	*r*(CO)	1.407	1.425	1.427	1.429	1.426	1.422	1.423
	r(OO)	1.383	1.442	1.400	1.392	1.402	1.411	1.408
	r(CH)	1.081	1.092	1.095	1.092	1.089	1.090	1.090
	r(CH′)	1.080	1.092	1.093	1.091	1.089	1.089	1.089
	r(CH")	1.084	1.096	1.097	1.095	1.092	1.093	1.092
	r(OBr)	1.800	1.977	1.994	2.012	1.979	1.932	1.926
	r(BrO′)	1.671	1.653	1.695	1.692	1.680	1.665	1.666
	∠(COO)	108.2	106.8	108.8	109.4	108.9	108.7	108.9
	∠(HCO)	110.5	110.8	110.8	110.6	110.7	111.0	110.7
	∠(H′CO)	104.9	104.3	104.7	104.7	104.7	104.7	104.5
	∠(H"CO)	110.8	110.8	110.3	110.6	110.7	111.0	110.8
	∠(OOBr)	110.5	108.0	111.6	113.4	112.1	111.9	112.2
	∠(OBrO′)	108.4	112.8	111.3	113.1	111.5	110.5	110.0
	∠(HCOO)	57.7	56.9	56.3	54.9	55.7	56.9	57.5
	∠(H′COO)	176.6	175.9	175.7	174.1	174.8	175.9	176.5
	∠(H"COO)	−65.0	−66.1	−66.3	−67.9	−67.3	−66.2	−65.6
	∠(COOBr)	99.3	88.9	85.8	88.7	90.6	92.7	92.2
	∠(OOBrO′)	75.3	72.9	73.7	76.9	76.7	78.1	77.4
CH_3OBrO_2	*r*(CO)	1.432	1.440	1.431	1.434	1.434	1.435	1.436
	r(CH)	1.079	1.090	1.094	1.091	1.089	1.088	1.088
	r(CH′)	1.079	1.094	1.096	1.093	1.090	1.090	1.089
	r(O′Br)	1.752	1.882	1.902	1.893	1.884	1.853	1.850
	r(BrO)	1.608	1.620	1.649	1.636	1.629	1.618	1.619
	∠(HCO)	104.5	104.7	104.8	104.5	104.6	104.8	104.5
	∠(H′CO)	110.1	111.0	111.3	111.2	111.1	111.0	111.0
	∠(COBr)	115.1	109.5	110.9	112.6	111.8	112.7	113.8
	∠(OBrO)	103.4	103.3	103.7	103.7	103.8	103.7	104.0
	∠(H′CO′Br)	180.0	180.0	180.0	180.0	180.0	180.0	180.0
	∠(HCOBr)	61.3	61.4	61.7	61.8	61.8	61.7	61.8
	∠(COBrO)	57.3	57.9	57.8	58.3	57.9	57.7	57.6
CH_3BrO_3	*r*(CBr)	1.921	1.941	2.000	1.984	1.989	1.976	1.976
	r(BrO)	1.600	1.615	1.644	1.629	1.622	1.609	1.612
	r(CH)	1.078	1.089	1.089	1.087	1.084	1.084	1.084
	∠(CBrO)	104.8	104.0	104.0	104.3	104.5	104.7	104.9
	∠(HCBr)	105.4	105.4	104.7	105.1	104.5	104.8	104.6
	∠(HCH)	113.2	113.2	113.8	113.5	114.0	113.7	113.8
	∠(OBrO)	113.7	114.3	114.3	114.1	114.0	113.8	113.6
	∠(HCBrO)	180.0	180.0	180.0	180.0	180.0	180.0	180.0

are three CH_3 stretches in CH_3OOOBr occurring at very high frequencies, and four CH_3 deformation modes occurring at lower frequencies. The O′−Br stretch in CH_3OOOBr occurs at a slightly lower frequency (530 cm^{-1}) than the O′−Br stretch in HOOOBr (584 cm^{-1}).

For CH_3OOBrO the most intense band is predicted, at the B3LYP theory level, to be the O−O stretch (ν_{11}) occurring at 826 cm^{-1}, and the least intense bands are predicted to be the CH_3 rock, ν_8 (1168 cm^{-1}); hydrogen wag, ν_{16} (180 cm^{-1}); and the CH_3 twist, ν_{17} (115 cm^{-1}). The C−O stretch, ν_9 (999 cm^{-1}), has a much larger frequency than the Br−O′ symmetric and asymmetric stretches, ν_{10} and ν_{12} (859 and 483 cm^{-1}), since the C−O bond is much shorter than the Br−O′ bond. The hydrogen wagging mode at 180 cm^{-1} present in CH_3OOBrO is absent in the CH_3OOOBr structure. The harmonic frequencies of CH_3OOBrO are similar to those of $HOOBrO$[16], with the exception of the CH_3 stretch and deformation modes and the C−O stretch in CH_3OOBrO that are absent in the HOOBrO structural form. The frequency band that clearly distinguishes CH_3OOBrO from CH_3OOOBr is the OOO′ bend occurring at 582 cm^{-1} in CH_3OOOBr, which is absent in CH_3OOBrO.

For CH_3OBrO_2, the most intense band is the Br−O asymmetric stretch, ν_{10}, positioned at 939 cm^{-1}, while the least intense band is the CH_3 symmetric deformation, ν_7, at 1175

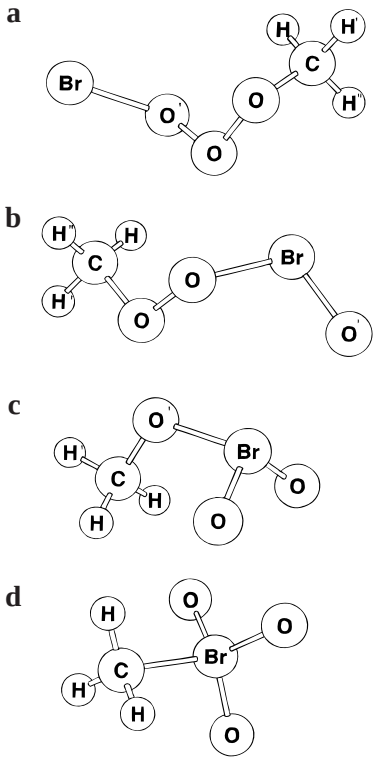

Figure 1. Minimum-energy structures for CH_3BrO_3 isomers (a) CH_3OOOBr, (b) CH_3OOBrO, (c) CH_3OBrO_2, and (d) CH_3BrO_3.

cm^{-1}. The hydrogen wagging mode, ν_{17}, occurs at 122 cm^{-1}, but has zero intensity. The Br−O symmetric and asymmetric stretches (896 and 939 cm^{-1}, respectively) occur at lower frequencies than the C−O stretch (969 cm^{-1}), consistent with the length of the Br−O bond being greater than the length of the C−O bond. The COBr bending mode occurs at 294 cm^{-1} and is a bit larger than the OBrO bending mode. The frequency modes that can clearly distinguish CH_3OBrO_2 from CH_3OOOBr are the O−O′ stretch and the OOO′ bend modes occurring in CH_3OOOBr.

The CH_3BrO_3 isomeric form possesses six ($\nu_7-\nu_{12}$) doubly degenerate modes. Its most intense band is the CH_3 rocking mode, ν_9, occurring at a frequency of 963 cm^{-1}. The least intense band is the CH_3 symmetric stretch, ν_1, at 3075 cm^{-1}, while the CH_3 symmetric deformation (ν_2), HCBrO torsion (ν_6), and CBrO bend (ν_{12}) modes possess no intensity. The C−Br stretch has a much smaller frequency (526 cm^{-1}) than the Br−O symmetric (856 cm^{-1}) and asymmetric (924 cm^{-1}) stretches, since the C−Br bond is longer than the Br−O bond (Table 1). A frequency mode that would distinguish CH_3BrO_3 from the CH_3OOOBr structure is the OBrO bend in CH_3BrO_3 occurring at 354 cm^{-1}.

B. Relative Energetics of CH_3BrO_3 Isomers. The calculated relative energies for the four minimum-energy isomers of CH_3BrO_3 are presented in Table 3. Using the B3LYP level of theory and different basis sets, the order of relative stability among the isomers (from most stable to least stable) is CH_3OOOBr > CH_3OBrO_2 > CH_3OOBrO > CH_3BrO_3. The relative energetic stability among the isomers is sensitive to electron correlation effects. It is also sensitive to the types of basis sets used to perform the computations. For instance, the relative energy difference between CH_3OOOBr and CH_3OBrO_2 at the B3LYP/6-311G(d,p) level of theory is 20.3 kcal mol^{-1}. Using the large 6-311++G(3df,3pd) basis set, the relative energy difference between the two structures decreases to 1.6 kcal mol^{-1}. In Table 3 are listed the relative energetics of the CH_3BrO_3 isomers calculated using G1 and G2 theories. Using the G2 theory, the order of relative stability of the CH_3BrO_3 isomeric forms is CH_3OBrO_2 > CH_3OOOBr > CH_3OOBrO > CH_3BrO_3, with CH_3OBrO_2 being the lowest energy structure. Previous studies conducted by Guha and Francisco[16] on the isomers of $HBrO_3$ have shown that G1 and G2 theories are more reliable in predicting the correct order of energies over the B3LYP level of theory. Thus, for the CH_3BrO_3 isomers, we believe that the order of energies predicted by the G1 and G2 theories is reasonable.

An isodesmic reaction scheme is used to estimate the heat of formation of CH_3OOOBr using G1, G2, and B3LYP energetics. Isodesmic reactions, which have been typically used to obtain the heats of formation for many molecules, are those in which the reactants and products contain the same types of bonds, i.e., the number of bonds broken and formed is conserved. An isodesmic reaction scheme requires that the heats of formation of all the molecules involved in the reaction to be known with the exception of the heat of formation of the particular isomer. Because of this property, errors in the energy that might occur due to defects in the basis set and electron correlation cancel, to a large extent. The isodesmic scheme used here is $CH_3OOOBr + 2HOH \rightarrow 2HOOH + CH_3OBr$. During the calculation of the heat of formation of CH_3OOOBr using the isodesmic scheme, literature values for the heats of formation of HOH (-57.10 ± 0.10 kcal mol^{-1}),[17] HOOH (-31.02 ± 0.05 kcal mol^{-1}),[17] and CH_3OBr (-5.4 kcal mol^{-1})[18] were used. Using these results we were able to calculate the heats of reaction. The results appear to be insensitive to both basis set and electron correlation effects, as shown in Table 4.

For CH_3OOOBr, the heat of formation is predicted to be 20.3 kcal mol^{-1} at the B3LYP level of theory, using the large 6-311++G(3df,3pd) basis set. Using the relative energies in Table 3 along with the heat of formation of CH_3OOOBr determined using the isodesmic results for the heats of formation of the CH_3BrO_3 isomers, we obtained a value of 34.4 kcal mol^{-1} for CH_3OOBrO, 21.9 kcal mol^{-1} for CH_3OBrO_2, and 68.9 kcal mol^{-1} for CH_3BrO_3. To further assess these results we have listed the G1 and G2 heats of formation of the isomers in Table 5. The G1 result for the heat of formation of CH_3OOOBr is 16.3 kcal mol^{-1}, and differs from the isodesmic result by 4.0 kcal mol^{-1}. The G2 value for the heat of formation of CH_3OOOBr is 16.2 kcal mol^{-1}, and agrees closely with its G1 heat of formation. Using G2 theory the heats of formation for CH_3OBrO_2, CH_3OOBrO, and CH_3BrO_3 were obtained as 10.6, 28.5, and 53.4 kcal mol^{-1}, respectively.

The G2 analysis provided here suggests that the lowest energy isomer is CH_3OBrO_2. The CH_3OOOBr structure is higher in energy than the CH_3OBrO_2 structure by 5.6 kcal mol^{-1}. The CH_3OOBrO and CH_3BrO_3 structural forms are higher in energy than CH_3OBrO_2 by 17.9 and 42.8 kcal mol^{-1}, respectively. The CH_3BrO_3 structure possesses the highest energy and, thus, the least stability.

At present, there are no experimental measurements to which the estimated heats of formation for the CH_3BrO_3 isomers can be compared. It would be useful to know the uncertainties associated with the present calculations. To estimate the possible uncertainties, we have calculated the error difference between the heats of formation determined with the G2 and the CCSD(T)/6-311++G(3df,3pd)//CCSD(T)/TZ2P methods for $HBrO_3$ isomers. The $HBrO_3$ system is structurally similar to the CH_3BrO_3 system, since the hydrogen atom in $HBrO_3$ is replaced by a methyl group to form CH_3BrO_3. Moreover, the CCSD(T)/6-

TABLE 2: Harmonic Frequencies (cm^{-1}) and Intensities (km mol^{-1}) of CH_3BrO_3 Isomers

				B3LYP/6-311++G(3df,3pd)	
species	mode no.	symmetry	mode description	frequencies	intensities
$CH_3OOO'Br$	1	a	CH_3 asymmetric stretch	3130	6
	2		CH_3 symmetric stretch	3116	17
	3		CH_3 symmetric stretch	3035	32
	4		CH_3 asymmetric deformation	1506	15
	5		CH_3 asymmetric deformation	1468	11
	6		CH_3 symmetric deformation	1446	1
	7		CH_3 symmetric deformation	1204	5
	8		CH_3 rock	1171	1
	9		CO stretch	991	58
	10		OO stretch	877	16
	11		OO′ stretch	715	26
	12		OOO′ bend	582	3
	13		O′Br stretch	530	13
	14		torsion	435	10
	15		OO′Br bend	254	7
	16		CH_3 twist	200	1
	17		torsion	125	2
	18		CH_3OOO' torsion	60	3
CH_3OOBrO'	1	a	CH_3 asymmetric stretch	3130	7
	2		CH_3 symmetric stretch	3096	26
	3		CH_3 symmetric stretch	3019	28
	4		CH_3 asymmetric deformation	1497	15
	5		CH_3 asymmetric deformation	1469	9
	6		CH_3 symmetric deformation	1449	3
	7		CH_3 symmetric deformation	1205	3
	8		CH_3 rock	1168	2
	9		CO stretch	999	53
	10		BrO symmetric stretch	859	24
	11		OO stretch	826	102
	12		BrO asymmetric stretch	483	8
	13		OOBr bend	476	3
	14		OBrO′ bend	290	5
	15		torsion	220	3
	16		H-wag	180	2
	17		CH_3 twist	115	2
	18		torsion	67	2
CH_3OBrO_2	1	a	CH_3 asymmetric stretch	3126	3
	2		CH_3 symmetric stretch	3118	9
	3		CH_3 symmetric stretch	3035	21
	4		CH_3 asymmetric deformation	1507	17
	5		CH_3 asymmetric deformation	1474	11
	6		CH_3 symmetric deformation	1452	3
	7		CH_3 symmetric deformation	1175	1
	8		CH_3 rock	1166	8
	9		CO stretch	969	82
	10		BrO asymmetric stretch	939	132
	11		BrO symmetric stretch	896	54
	12		O′Br stretch	486	82
	13		OBrO bend	433	21
	14		OBrO bend	355	10
	15		COBr bend	294	10
	16		OBrO bend	211	12
	17		H-wag	122	0
	18		torsion	48	7
CH_3BrO_3	1	a_1	CH_3 symmetric stretch	3075	2
	2		CH_3 symmetric deformation	1288	0
	3		BrO symmetric stretch	856	40
	4		CBr stretch	526	14
	5		OBrO bend	367	51
	6	a_2	HCBrO torsion	141	0
	7	e	CH_3 asymmetric stretch	3210	4
	8		CH_3 asymmetric deformation	1437	9
	9		CH_3 rock	963	86
	10		BrO asymmetric stretch	924	39
	11		OBrO bend	354	16
	12		CBrO bend	231	0

311++G(3df,3pd)//CCSD(T)/TZ2P method has, generally, been able to predict heats for formation for closed-shell systems with a ±2 kcal mol^{-1} uncertainty. We find that the rms error between the G2 and CCSD(T) heats of formation for the $HBrO_3$ isomers is 7.0 kcal mol^{-1}. This suggests that the G2 estimates for the CH_3BrO_3 isomers have a probable uncertainty of ±7 kcal mol^{-1} associated with each determination.

C. Comparison of Relative Stability of $XBrO_3$ (X = H, CH_3) Isomers. Figure 2 shows a comparison of the heats of formation of CH_3BrO_3 isomers with the $HBrO_3$ isomers,

TABLE 3: Total and Relative Energies for CH_3BrO_3 Species

levels of theory	species			
	CH_3OOOBr	CH_3OOBrO	CH_3OBrO_2	CH_3BrO_3
	Total Energies (hartrees)			
B3LYP/6-31G(d)	−2837.057 22	−2837.022 72	−2837.026 94	−2836.941 22
B3LYP/6-311G(d,p)	−2839.574 69	−2839.53 600	−2839.542 32	−2839.462 85
B3LYP/6-311G(2d,2p)	−2839.583 08	−2839.549 65	−2839.560 00	−2839.478 35
B3LYP/6-311G(2df,2p)	−2839.592 26	−2839.563 01	−2839.582 77	−2839.506 47
B3LYP/6-311++G(3df,3pd)	−2839.607 73	−2839.584 55	−2839.605 10	−2839.529 55
G1	−2837.575 00	−2837.555 28	−2837.58206	−2837.509 85
G2	−2837.582 86	−2837.563 35	−2837.591 84	−2837.523 66
	Relative Energies (kcal mol^{-1})[a]			
B3LYP/6-31G(d)	0.0	21.2	18.9	72.3
B3LYP/6-311G(d,p)	0.0	23.9	20.3	69.7
B3LYP/6-311G(2d,2p)	0.0	20.6	14.4	65.2
B3LYP/6-311G(2df,2p)	0.0	17.9	5.9	53.3
B3LYP/6-311++G(3df,3pd)	0.0	14.1	1.6	48.6
G1	0.0	12.4	−4.4	40.9
G2	0.0	12.3	−5.6	37.2

[a] Relative energies are corrected for zero-point energy using B3LYP/6-311++G(3df,3pd) frequencies.

TABLE 4: Isodesmic Heats of Reaction (kcal mol^{-1}) and Heats of Formation (kcal mol^{-1}) of CH_3OOOBr

levels of theory	HOH	CH_3OBr	HOOH	CH_3OOOBr	$\Delta H^0_{r,0}$ $CH_3OOOBr + 2HOH \rightarrow 2HOOH + CH_3OBr$	$H^0_{f,0}$ (CH_3OOOBr)
B3LYP/6-31G(d)	−76.408 95	−2686.776 46	−151.533 21	−2837.057 22	22.9	23.9
B3LYP/6-311G(d,p)	−76.447 45	−2689.252 10	−151.591 85	−2839.574 69	23.9	22.9
B3LYP/6-311G(2d,2p)	−76.452 12	−2689.254 86	−151.599 08	−2839.583 08	24.2	22.6
B3LYP/6-311G(2df,2p)	−76.452 76	−2689.260 83	−151.601 37	−2839.592 26	24.2	22.6
B3LYP/6-311++G(3df,3pd)	−76.464 51	−2689.272 48	−151.613 19	−2839.607 73	26.5	20.3
G1	−76.328 34	−2687.461 55	−151.362 92	−2837.575 00	30.5	16.3
G2	−76.332 05	−2687.470 99	−151.365 78	−2837.582 86	30.6	16.2

TABLE 5: Heats of Formation (kcal mol^{-1}) for CH_3BrO_3 Species

species	B3LYP/6-311++ G(3df,3pd)	G1	G2
CH_3OOOBr	20.3	16.3	16.2
CH_3OOBrO	34.4	28.7	28.5
CH_3OBrO_2	21.9	11.9	10.6
CH_3BrO_3	68.9	57.2	53.4

calculated previously by Guha and Francisco.[16] Such a comparison indicates that the most stable isomeric form is $HOBrO_2$ with a 5.7 kcal mol^{-1} heat of formation, while the least stable isomer is $HBrO_3$ with a 71.6 kcal mol^{-1} heat of formation. The order of energy levels for CH_3BrO_3 isomers using the G2 theory follows the same pattern as that of the $HBrO_3$ isomers, i.e., CH_3OBrO_2 > CH_3OOOBr > CH_3OOBrO > CH_3BrO_3, with CH_3OBrO_2 being the most stable structural form. The G2 heat of formation of $HOBrO_2$ is 5.7 kcal mol^{-1}, and increases by 4.9 kcal mol^{-1} when the hydrogen atom in $HOBrO_2$ is replaced by a methyl group to form CH_3OBrO_2 (which is the structural form that possesses the most stability after $HOBrO_2$). It is very important to consider the type of bonding that exists within each isomer to determine the relative stability among them. The differences between the heats of formation among $HOOOBr$ and CH_3OOOBr, $HOOBrO$ and CH_3OOBrO, and $HBrO_3$ and CH_3BrO_3 are 2.6, 2.3, and 18.2 kcal mol^{-1}, respectively. Interestingly enough, the CH_3BrO_3 structural form lies at a significantly lower energy level than the $HBrO_3$ structural form.

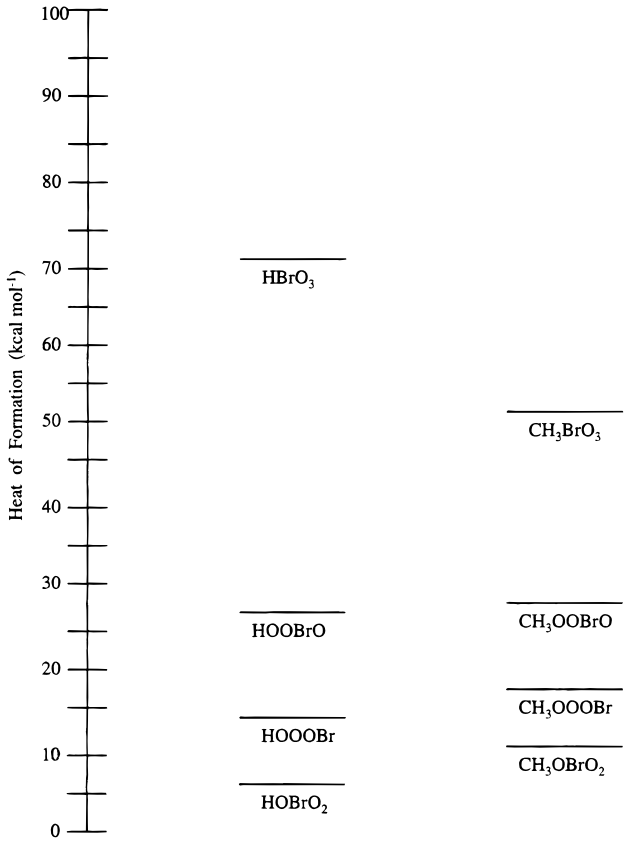

Figure 2. Relative energetics of $XBrO_3$ (X = H, CH_3) isomers.

IV. Conclusion

The equilibrium structures, vibrational and electronic spectra, relative energetics, and heats of formation of the CH_3BrO_3 isomers have been investigated with the B3LYP *ab initio* electronic structure method in conjugation with the 6-31G(d), 6-311G(d,p), 6-311G(2d,2p), 6-311G(2df,2p), and 6-311++G(3df,3pd) basis sets. The CH_3OBrO_2 structure was found to be

the most stable form among the isomers with an estimated heat of formation of 10.6 kcal mol^{-1}. The heats of formation of CH_3OOOBr, CH_3OOBrO, and CH_3BrO_3 are 16.2, 28.5, and 53.4 kcal mol^{-1}, respectively.

References and Notes

(1) Anderson, J. G.; Toohey, D. W.; Brune, W. H. *Science* **1991**, *251*, 39.

(2) Salawitch, R. J.; McElroy, M. B.; Yatteau, J. H.; Wofsy, S. C.; Schoeberl, M. R.; Lait, L. R.; Newman, P. A.; Chan, K. R.; Loewenstein, M.; Podolske, J. R.; Strahan, S. E.; Proffitt, M. H. *Geophys. Res. Lett.* **1990**, *17*, 561.

(3) Yung, Y. L.; Pinto, J. P.; Watson, R. T.; Sander, S. P. *J. Atmos. Sci.* **1980**, *37*, 339.

(4) World Metereological Organization. Scientific Assessment of Ozone Depletion; National Aeronautics and Space Administration, U.S. Government Printing Office: Washington, DC, 1994.

(5) Vogt, R.; Crtuzen, P. J.; Sander, R. *Nature* **1996**, *383*, 327.

(6) Poulet, G.; Pirre, M.; Maguin, F.; Ramaroson, R.; Le Bras, G. *Geophys. Res. Lett.* **1992**, *19*, 2305.

(7) Larichev, M.; Maguin, F.; Le Bras, G.; Poulet, G. *J. Phys. Chem.* **1995**, *99*, 15911.

(8) Elrod, M. J.; Meads, R. F.; Lipson, J. B.; Seeley, J. V.; Molina, M. J. *J. Phys. Chem.* **1996**, *100*, 5808.

(9) Fan, S. M.; Jacob, D. J. *Nature* **1992**, *359*, 522.

(10) Crutzen, P. J.; Muller, R.; Bruhl, C.; Peter, T. *Geophys. Res. Lett.* **1992**, *19*, 1113.

(11) Aranda, A.; Le Bras, G.; La Verdet, G.; Poulet, G. *Geophys. Res. Lett.* **1997**, *24*, 2745.

(12) Frisch, M. J.; Trucks, G. W.; Schlegel, H. B.; Gill, P. M. W.; Johnson, B. G.; Robb, M. A.; Cheeseman, J. R.; Keith, T.; Petersson, G. A.; Montgomery, J. A.; Raghavachari. K.; Al-Laham, M. A.; Zakrzewski, V. G.; Ortiz, J. V.; Foresman, J. B.; Cioslowski, J.; Stefanov, B. B.; Nanayakkara, A.; Challacombe, M.; Peng, C. Y.; Ayala, P. Y.; Chen, W.; Wong, M. W.; Andres, J. L.; Replogle, E. S.; Gomperts, R.; Martin, R. L.; Fox, D. J.; Binkley, J. S.; Defrees, D. J.; Baker, J.; Stewart, J. P.; Head-Gordon, M.; Gonzales, C.; Pople, J. A. *GAUSSIAN 94*, Revision D.2; Gaussian, Inc.: Pittsburgh, PA, 1995.

(13) Lee, C.; Yang, W.; Parr, R. G. *Phys. Rev. B* **1988**, *41*, 785.

(14) Pople, J. A.; Head-Gordon, M. D.; Fox, J.; Raghavachari, K.; Curtiss, L. A. *J. Chem. Phys.* **1989**, *90*, 5622.

(15) Curtiss, L. A.; Raghavachari, K.; Trucks, G. W.; Pople, J. A. *J. Chem. Phys.* **1991**, *94*, 7221.

(16) Guha S.; Francisco, J. S. *J. Phys. Chem. A* **1998**, *102*, 2072.

(17) Chase, M. W.; Davies, C. A.; Downey, J. R.; Frurip, D. J.; McDonald, R. A.; Syverud, A. N. *J. Phys. Chem. Ref. Data, Suppl.* **1985**, *1*.

(18) Guha S.; Francisco, J. S. *J. Phys. Chem. A* **1998**, *102 (48)*, 9970.